Acta Crystallographica Section F
Structural Biology and Crystallization Communications
ISSN 1744-3091

Crystallization and preliminary X-ray analysis of 4-diphosphocytidyl-2-*C*-methyl-D-erythritol kinase (IspE) from *Mycobacterium tuberculosis*

Shan Shan[a] and Xuehui Chen[a,b]*

[a]Structural Biology Laboratory, Tsinghua University, Beijing 100084, People's Republic of China, and [b]National Laboratory of Macromolecules, Institute of Biophysics, Chinese Academy of Science, Beijing 100101, People's Republic of China

Correspondence e-mail: chenxh@pku.edu.cn

Received 17 January 2011
Accepted 23 May 2011

The 4-diphosphocytidyl-2-*C*-methyl-D-erythritol kinase (IspE) from *Mycobacterium tuberculosis*, an enzyme from the 2-*C*-methyl-D-erythritol 4-phosphate (MEP) pathway, is crucial and essential for the survival of this pathogenic bacterium. IspE catalyzes the conversion of 4-diphosphocytidyl-2-*C*-methyl-D-erythritol (CDP-ME) to 4-diphosphocytidyl-2-*C*-methyl-D-erythritol 2-phosphate (CDP-ME2P) in an ATP-dependent manner. Solving the crystal structure of *M. tuberculosis* IspE will shed light on its structural details and mechanism of action and may provide the basis for the future design of drugs for the treatment of multidrug-resistant and extremely drug-resistant *M. tuberculosis* strains. Recombinant *M. tuberculosis* IspE was crystallized at 291 K using NaCl or Li_2SO_4 as a precipitant. A 2.1 Å resolution native data set was collected from a single flash-cooled crystal (100 K) belonging to space group $P2_12_12_1$, with unit-cell parameters a = 52.5, b = 72.3, c = 107.3 Å. One molecule was assumed per asymmetric unit, which gives a Matthews coefficient of 3.4 Å^3 Da^{-1} with 63% solvent content.

1. Introduction

Isoprenoids participate in many important biological functions such as electron transport, hormone-based signalling and the biosynthesis of structural components of the cell wall of some pathogens. Indeed, isoprenoids play an essential role in the life cycle of mycobacteria. Thus, better understanding the isoprenoid-biosynthesis pathway may aid in the discovery of potential drug targets for the treatment of mycobacterial infections (Brennan & Crick, 2007; Gershenzon & Dudareva, 2007; Edwards & Ericsson, 1999; Mikusová *et al.*, 1996).

The 2-*C*-methyl-D-erythritol 4-phosphate (MEP) pathway is the synthesis route for the isoprenoid precursor isopentenyl diphosphate (IPP) and its isomer dimethylallyl diphosphate (DMAPP) in bacteria, plant plastids and several pathogenic microorganisms (e.g. *Mycobacterium tuberculosis*, *Plasmodium falciparum* and *Vibrio cholerae*; Eisenreich *et al.*, 2004; Eoh, Narayanasamy *et al.*, 2009). The enzymes involved in the MEP pathway are potential drug targets because they are absent in humans and are essential for bacterial survival (Testa & Brown, 2003; Rohmer, 1998; Hasan *et al.*, 2006; de Ruyck & Wouters, 2008; Eoh, Brennan *et al.*, 2009). IspE is the fourth enzyme in the MEP pathway and is responsible for catalyzing the ATP-dependent phosphorylation of 4-diphosphocytidyl-2-*C*-methyl-D-erythritol (CDP-ME) to give 4-diphosphocytidyl-2-*C*-methyl-D-erythritol 2-phosphate (CDP-ME2P); it was recently identified to be essential in *M. smegmatis* (Eisenreich *et al.*, 2004). Sequence-alignment results revealed that IspE belongs to the galactose/homoserine/mevalonate/phosphomevalonate (GHMP) kinase superfamily (Zhou *et al.*, 2000; Cheek *et al.*, 2002) and the sequence similarities among IspE family members suggest conservation of overall structure and enzymatic mechanism. To date, crystal structures of IspE from *Escherichia coli*, *Aquifex aeolicus* and *Thermus thermophilus* have been reported (Wada *et al.*, 2003; Miallau *et al.*, 2003; Sgraja *et al.*, 2008), but the structure of *M. tuberculosis* IspE remains elusive.

Here, we report the expression, purification, crystallization and preliminary X-ray analysis of *M. tuberculosis* IspE. We believe that our results may provide a basis for further structural investigation of *M. tuberculosis* IspE which will provide structural details for the design of structure-based anti-*M. tuberculosis* drugs and may provide

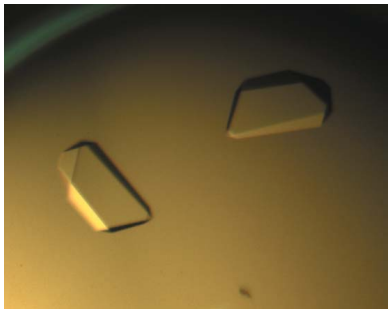

insight for future drug discovery to treat multidrug-resistant (MDR) and extremely drug-resistant (XDR) strains.

2. Materials and methods

2.1. Expression and purification of recombinant *M. tuberculosis* IspE

The gene encoding the full-length 306-amino-acid IspE was cloned into the *Nde*I and *Xho*I restriction sites of the pET-28a vector (Novagen) to include an N-terminal His tag and thrombin protease cleavage site. *E. coli* cells transformed with this vector were grown with shaking for 4–5 h at 310 K in 1 l LB medium containing 50 µg ml^{-1} kanamycin until the OD_{600} reached 0.4–0.6. Isopropyl β-D-1-thiogalactopyranoside was then added to a final concentration of 0.3 m*M* to induce IspE expression for 16–20 h at 289 K. The cells were harvested, resuspended in 20 m*M* Tris buffer containing 500 m*M* NaCl, 5 m*M* β-mercaptoethanol and 10 m*M* imidazole pH 8.0, lysed by sonication on ice for 10 min and clarified by centrifugation at 16 000*g* for 35 min at 277 K. The supernatant was loaded onto an Ni–NTA column equilibrated with the same buffer. After removing nonspecifically bound protein by washing with five column volumes of 20 m*M* Tris buffer containing 30 m*M* imidazole, the target protein was eluted with 20 m*M* Tris buffer containing 100 m*M* imidazole. The eluted protein was pooled with thrombin protease and dialyzed against 20 m*M* Tris–HCl pH 7.0, 50 m*M* NaCl and 1 m*M* DTT at 277 K overnight to cleave the N-terminal 6×His tag. Finally, the solution containing IspE was reloaded onto the Ni–NTA column to remove the cleaved tag.

Recombinant protein was further purified to homogeneity using a pre-packed Resource Q anion-exchange column (GE Healthcare) and a Superdex 200 gel-filtration column (GE Healthcare) according to the manufacturer's recommendations using Tris buffer pH 7.0 containing 1 m*M* DTT. Fractions were analyzed by SDS–PAGE and IspE purity was confirmed to be >95%. The purified protein was ultimately concentrated to 15 mg ml^{-1} in 20 m*M* Tris–HCl pH 7.0, 50 m*M* NaCl and 5 m*M* DTT with Amicon Ultra spin columns (5 kDa exclusion size) from Millipore.

2.2. Crystallization

Initial crystallization conditions were screened *via* the hanging-drop vapour-diffusion method at 289 K. Drops consisting of 1 µl protein solution (15 mg ml^{-1}) and 1 µl well solution were equilibrated against 0.2 ml well solution. Commercially available crystallization screens (Index HT, SaltRx and Crystal Screen HT from Hampton Research) were employed and crystallization trays were set up in Linbro plates.

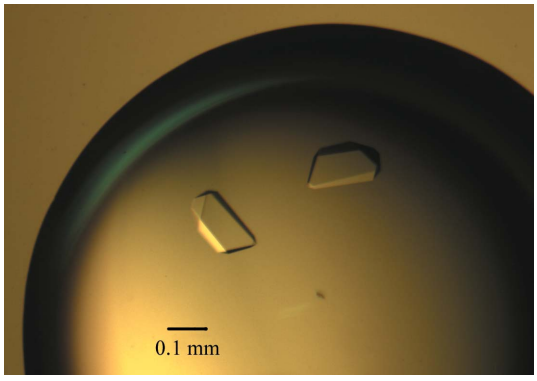

Figure 1
Single crystals of *M. tuberculosis* IspE.

Table 1
Statistics of data collection and processing.

Values in parentheses are for the highest resolution shell.

Space group	$P2_12_12_1$
Unit-cell parameters (Å, °)	a = 52.5, b = 72.3, c = 107.3, $\alpha = \beta = \gamma$ = 90
Wavelength (Å)	1.0000
Resolution range (Å)	50.0–2.1 (2.2–2.1)
Total reflections	153128 (12911)
Unique reflections	24569 (2391)
Multiplicity	4.7 (4.5)
Average $I/\sigma(I)$	13.4 (2.4)
R_{merge}† (%)	9.2 (61.5)
Data completeness (%)	99.8 (99.0)
Molecules per asymmetric unit	1
V_M (Å^3 Da^{-1})	3.4
Solvent content (%)	63

† $R_{merge} = \sum_{hkl}\sum_i |I_i(hkl) - \langle I(hkl)\rangle| / \sum_{hkl}\sum_i I_i(hkl)$.

After one week, rectangular-shaped but small and markedly twinned crystals were observed using apoprotein under aerobic conditions with 0.1 *M* Bis-Tris propane pH 7.0, 3.2 *M* NaCl or with 0.1 *M* Bis-Tris propane pH 7.0, 1.5 *M* Li_2SO_4. The crystals grown using Li_2SO_4 were chosen for optimization owing to their better diffraction. These crystals belonged to an orthorhombic space group and had poor diffraction quality. Although several rounds of optimization produced larger crystals belonging to the same lattice, the resolution of these crystals remained limited to 3.5 Å. Eventually, streak-seeding was used to optimize the crystals to final dimensions of 80 × 80 × 100 µm (Fig. 1) with a resolution of 2.1 Å (Fig. 2). The crystals were then soaked in a cryoprotectant solution consisting of the reservoir solution and 20%(*v*/*v*) glycerol and flash-frozen in liquid nitrogen for X-ray diffraction data collection.

2.3. Data collection and X-ray crystallographic analysis

Initial diffraction data were collected on an R-AXIS IV^{++} image-plate detector (Rigaku) at 100 K using a Rigaku FR-E rotating-anode home X-ray generator operated at 45 kV and 45 mA (λ = 1.000 Å). The high-resolution native data set used for structure determination was collected on beamline BL-17 at Photon Factory with an ADSC Q270 CCD detector. The data were collected at a wavelength of 1.0 Å. Crystals were mounted on a nylon loop and flash-cooled in a nitrogen-gas cryostream at 100 K. A total of 180 frames of data were collected with a 0.5° oscillation range. All intensity data were indexed, integrated and scaled with the *HKL*-2000 package (Otwinowski & Minor, 1997). Complete data-collection statistics are given in Table 1.

3. Results and discussion

Streak-seeding proved to be crucial in obtaining diffraction-quality crystals. Microcrystals from a previous batch were transferred to 100 µl well solution and shaken. A cat whisker was used for streak-seeding: it was touched into the solution containing the crystal pieces and then used to draw a streak line across a pre-equilibrated drop consisting of 1 µl protein solution (15 mg ml^{-1}) and 1 µl well solution. Single crystals appeared 3–4 d after seeding and diffracted to ∼2.1 Å resolution.

Soaking was used in order to determine the details of the interaction of IspE with its substrates CDP-ME and AMP-PNP, which is an analogue of ATP. Crystals grown using either Li_2SO_4 or NaCl were

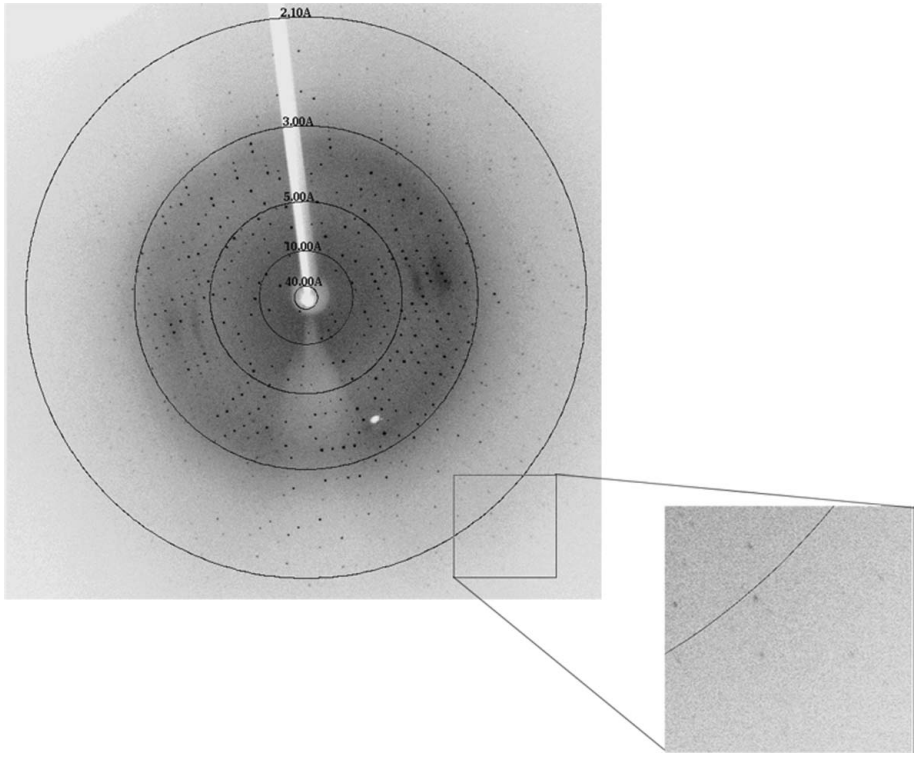

Figure 2
Typical diffraction pattern of the apo IspE crystal. The exposure time was 2 s, with an oscillation range per frame of 0.5°.

transferred to soaking solutions containing the substrates. Diffraction data were collected after soaking. Initial electron-density maps were calculated in order to check for substrate binding. Clear density corresponding to the substrates could be observed after a 24 h soak of crystals grown using Li_2SO_4 with CDP-ME or AMP-PNP. We also tried to cocrystallize IspE with both of the substrates, but did not observe any density at the position occupied by the substrates. A comparison of data sets collected from an apo crystal and a soaked crystal demonstrated that little change in the unit-cell parameters had occurred during the substrate and cofactor soaking.

Molecular replacement was performed with the crystal structure of *T. thermophilus* IspE (PDB entry 1uek; 38% sequence identity to *M. tuberculosis* IspE; Wada *et al.*, 2003) as the initial search model. This procedure was performed using *Phaser* (McCoy *et al.*, 2007). The high rotation and translation *Z*-score values of 6.2 and 9.7 suggested that the correct solution had been obtained. Initial rounds of rigid-body refinement and energy minimization in *PHENIX* (Adams *et al.*, 2002) resulted in an R_{work} of 37% (R_{free} = 42%). Manual model building and refinement are currently in progress and structural details will be presented elsewhere.

We thank the staff of the BSRF and the SSRF for their technical assistance. This work was supported by the National Natural Science Foundation of China (grant Nos. 30770516 and 30870486) and the National Major Projects (grant Nos. 2009ZX09311-001 and 2009ZX10004-304).

References

Adams, P. D., Grosse-Kunstleve, R. W., Hung, L.-W., Ioerger, T. R., McCoy, A. J., Moriarty, N. W., Read, R. J., Sacchettini, J. C., Sauter, N. K. & Terwilliger, T. C. (2002). *Acta Cryst.* D**58**, 1948–1954.
Brennan, P. J. & Crick, D. C. (2007). *Curr. Top. Med. Chem.* **7**, 475–488.
Cheek, S., Zhang, H. & Grishin, N. V. (2002). *J. Mol. Biol.* **320**, 855–881.
Edwards, P. A. & Ericsson, J. (1999). *Annu. Rev. Biochem.* **68**, 157–185.
Eisenreich, W., Bacher, A., Arigoni, D. & Rohdich, F. (2004). *Cell. Mol. Life Sci.* **61**, 1401–1426.
Eoh, H., Brennan, P. J. & Crick, D. C. (2009). *Tuberculosis*, **89**, 1–11.
Eoh, H., Narayanasamy, P., Brown, A. C., Parish, T., Brennan, P. J. & Crick, D. C. (2009). *Chem. Biol.* **16**, 1230–1239.
Gershenzon, J. & Dudareva, N. (2007). *Nature Chem. Biol.* **3**, 408–414.
Hasan, S., Daugelat, S., Rao, P. S. & Schreiber, M. (2006). *PLoS Comput. Biol.* **2**, e61.
McCoy, A. J., Grosse-Kunstleve, R. W., Adams, P. D., Winn, M. D., Storoni, L. C. & Read, R. J. (2007). *J. Appl. Cryst.* **40**, 658–674.
Miallau, L., Alphey, M. S., Kemp, L. E., Leonard, G. A., McSweeney, S. M., Hecht, S., Bacher, A., Eisenreich, W., Rohdich, F. & Hunter, W. N. (2003). *Proc. Natl Acad. Sci. USA*, **100**, 9173–9178.
Mikusová, K., Mikus, M., Besra, G. S., Hancock, I. & Brennan, P. J. (1996). *J. Biol. Chem.* **271**, 7820–7828.
Otwinowski, Z. & Minor, W. (1997). *Methods Enzymol.* **276**, 307–326.
Rohmer, M. (1998). *Prog. Drug Res.* **50**, 135–154.
Ruyck, J. de & Wouters, J. (2008). *Curr. Protein Pept. Sci.* **9**, 117–137.
Sgraja, T., Alphey, M. S., Ghilagaber, S., Marquez, R., Robertson, M. N., Hemmings, J. L., Lauw, S., Rohdich, F., Bacher, A., Eisenreich, W., Illarionova, V. & Hunter, W. N. (2008). *FEBS J.* **275**, 2779–2794.
Testa, C. A. & Brown, M. J. (2003). *Curr. Pharm. Biotechnol.* **4**, 248–259.
Wada, T., Kuzuyama, T., Satoh, S., Kuramitsu, S., Yokoyama, S., Unzai, S., Tame, J. R. & Park, S.-Y. (2003). *J. Biol. Chem.* **278**, 30022–30027.
Zhou, T., Daugherty, M., Grishin, N. V., Osterman, A. L. & Zhang, H. (2000). *Structure*, **8**, 1247–1257.